CIS I - Programming Assignment 1 Report

Shreya Terala & Yvonne Zhang

January 16, 2026

1 Introduction

This report will focus on the tasks presented in Assignment 1, including the development of mathematical tools and subroutines for the calibration, registration, and tracking of a stereotactic navigation system using an electromagnetic position tracking device [1]. All programs were written in MATLAB for this project and will be used for all subsequent programming assignments.

2 Mathematical Approach

2.1 Terms and Setup

This section covers the variables and terminology used in the stereotactic navigation system problem scenario [1]. Diagrams were recreated for the team's comprehension.

2.1.1 Registration Algorithm

The setup includes a calibration object moving in the workspace, an optical tracker and the EM tracker base. The following variables define the stereotactic navigation system system and the workspace.

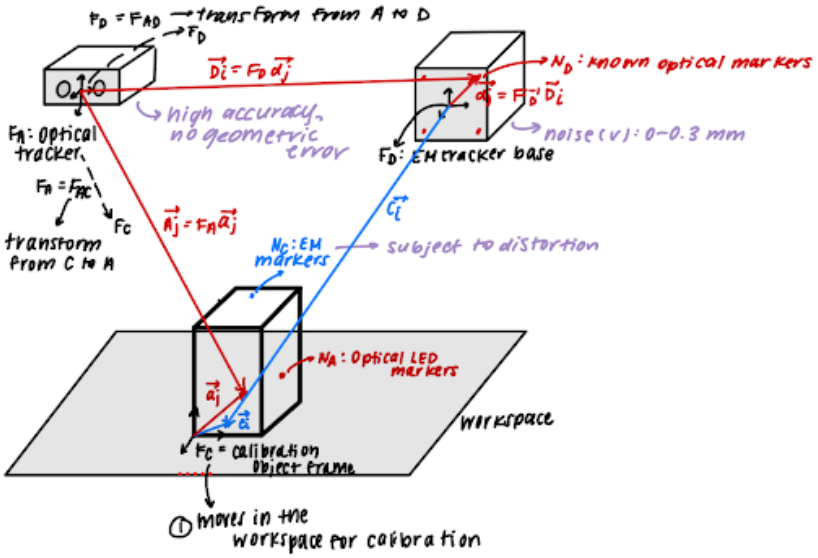

Figure 1: Registration System Setup

Error v = 0 to 0.3 mm
N_C - Calibration object EM markers
N_A - Calibration object optical LED markers
N_D - Optical markers in the EM tracking system

F_C - Frame calibration object coordinate system
F_A - Frame transformation from F_C to frame A (optical tracker)
F_D - Frame transformation from frame A (optical tracker) to frame D (EM tracker base)

C_i - Positions from frame D (EM tracker base) to EM markers on the calibration object
c_i - Known positions relative to F_C for i = $1 \dots N_C$
A_j - Positions from frame A (optical tracker) to optical LED markers on the calibration object
a_j - Position of optical markers relative to F_C frame on calibration object
D_j - Positions from frame A (optical tracker) to optical markers on EM base markers (N_D)
d_j - Positions of optical markers on the EM tracker base relative to frame D

Calibration data sample frame - position of the calibration object in the workspace, optical markers, and EM markers $[D_1, \dots, D_{N_D}, A_1, \dots, A_{N_A}, C_1, \dots, C_{N_C}]$

2.1.2 Pivot Calibration Method

Two pointer probes are used, one with LED markers and one with electromagnetic (EM) markers with unknown positions and orientations with respect to the EM tracker system. The pivot calibrations of each probe are given using the dimpled posts in the workspace. The following variables define the calibration probe systems.

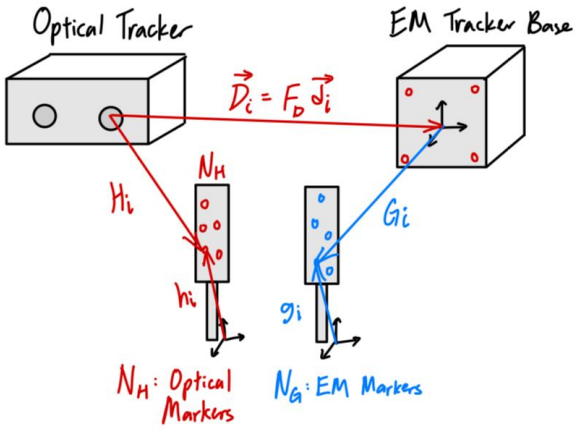

Figure 2: Pivot Calibration System Setup

N_H - LED markers unknown with fixed position h_i
N_G - EM markers unknown with fixed position g_i

The pivot calibration data at each post are given as:
Optical probe calibration: $[D_1, \dots, D_{N_D}, H_1, \dots, H_{N_H}]$
EM probe calibration: $[G_1, \dots, G_{N_G}]$

2.2 Cartesian Math Package

MATLAB's Symbolic Math Toolbox was used as the Cartesian math package for 3D points, rotations, and frame transformations [2].

Basic mathematical operations for the matrices were used, such as addition, matrix multiplication, and matrix transpose using single quotes ('). These operations were used throughout the assignment.

From Matlab's core numerical linear algebra libraries, the svd function performs a singular value decomposition of matrix H, such that [U,S,V] = svd(H) is used to solve $H = USV^T$ [3]. Singular value decomposition is used to solve for the covariance matrix in its matrix-vector product components. This includes the two orthogonal matrix U and V with columns formed by left and right singular vectors

of H respectively. S is a diagonal matrix containing the singular values of H [4]. This decomposition of the covariance will be utilized to determine the rotation matrix.

The lsqr function is used to solve the system of linear equations using the iterative least squares method. It solves the system by approximating $Ax \approx b$ by minimizing the Euclidean norm of the residual of [5]:

$$x = min_x||b - Ax||_2 \tag{1}$$

The least squares algorithm is an adaptation of the conjugate gradient method for rectangular matrices, where $Ax = b$ produces the same residuals as the conjugate gradient for the normal equation $A^T Ax = A^T b$, without forming the explicit $A^T A$ that results in superior numerical stability [6]. Note, the lsqr function will use a tolerance of $1e - 6$, which is sufficiently stable for our use case [6].

3 Algorithmic Steps

3.1 Reading Data Files

Algorithms were developed to read the provided data files by extracting the locations of the markers and their corresponding locations in each frame. The calibration data for frames D, A and C, is extracted using the function "read_cal_data.m". The pivot calibration data for the EM probe with respect to the EM tracker base is extracted using the function "read_em_pivot_data.m". The pivot calibration data for the optical probe with respect to the optical tracker base utilizing data from H and D is extracted using the function "read_optical_pivot_data.m".

The input is the string of the reading filepath. For "read_em_pivot_data.m" and "read_optical_pivot_data.m" functions, the string for empivot and optpivot is called upon to parse the uppercase X_i values. For "read_cal_data.m", there are two sets of data: calbody for the lowercase x_i markers and calreadings for the uppercase X_i coordinates.

The output for all files is the parsing of each file's header to use for all functions and algorithms of this project. For X_i, it is returned in the form of $N_{markers} \times 3 \times N_{frames}$ for each respective frame F_X. Notes that for calibration, x_i sets return $N_{markers} \times 3$ values.

The data reading algorithm first reads the data file using the function readmatrix. The first row of each file is split for "," to parse the number of each marker as according to the "Data file formats" section in the assignment [1].

The number of rows for each frame is partitioned from the heading and each frame's data block is extracted for each marker group in 3D arrays. Each frame's corresponding transformations (D, A, C, G and H) can be individually accessed for the project algorithms.

3.2 3D Point Set Registration Algorithm

A primary function, "point_cloud_registration.m", was developed to register the correspondence between the two 3D point sets. This function accepts two sets of corresponding points and returns the aligning transformation matrix using Arun's method [5]. The output is the rotation matrix and the translation vector that form the frame transformation matrix.

The following will use the lower case x_i for the calibration markers vector and X_i for the positions of the markers. This can correspond to all variables A, C, D, G, and H used in this assignment. Note that a similar algorithmic approach was taken for the "pivot_calibration.m" function to determine the transformations of each frame [k] of F_G.

First, the inputs from the data reading function is allocated to variables x_i and X_i for calibration markers and calibration frames readings respectively. The size of both markers and frames are also stored. Arun's method is used to find the optimal frame transformation in closed form to estimate the frame transformation that best aligns the set of known x_i object points with corresponding 3D points

X_i for each frame. For each frame, the following are solved to form the $SE(3)$ frame transformation [5]:

$$X_i \approx Rx_i + t, \quad R \in SO(3), \quad t \in R^3 \tag{2}$$

for $i = 1, ..., N$ in each frame.

Next, the translation is removed for centroid alignment to isolate the rotation from the translation effects of the transformation. The centroids of both point sets are calculated:

$$\bar{x} = \frac{1}{N}\sum_{i=1}^{N} x_i, \quad \bar{X} = \frac{1}{N}\sum_{i=1}^{N} X_i \tag{3}$$

The centroids are subtracted from each data point to obtain the centered coordinates:

$$x_i' = x_i - \bar{x}, \quad X_i' = X_i - \bar{X} \tag{4}$$

The optimal rotation is determined by minimizing the following equation with translation effects removed [5]:

$$\min_{R \in \mathrm{SO}(3)} \sum_{i=1}^{N} \left\| X_i' - Rx_i' \right\|^2 \tag{5}$$

By expanding the squared norm:

$$\left\| X_i' - Rx_i' \right\|^2 = \left(X_i' - Rx_i'\right)^T \left(X_i' - Rx_i'\right) = \left\|X_i'\right\|^2 + \left\|Rx_i'\right\|^2 - 2\left(X_i'\right)^T Rx_i' \tag{6}$$

where rotation has no effect inside a norm for $||Rx_i'||^2 = ||x_i'||^2$, and $||X_i'||^2$ and $||x_i'||^2$ are independent of rotation, then:

$$\min_R \sum_i \left\| X_i' - Rx_i' \right\|^2 \longleftrightarrow \max_R \sum_i \left(X_i'\right)^T Rx_i' \tag{7}$$

which identifies the covariance matrix that is defined as,

$$H = \sum_{i=1}^{N} \left(x_i'\right)\left(X_i'\right)^\top = \left(x_i'\right)\left(X_i'^\top\right) \tag{8}$$

The covariance matrix H is the correlation between the two centered point sets by encapsulating how the two sets are aligned in orientation. Its singular value decomposition can be found using the svd function for the following equation:

$$H = USV^\top \tag{9}$$

The optimal rotation is solved by utilizing the diagonal matrix for the weight of the diagonal entries of the covariance matrix H, therefore the weights of the mapping from x_i to X_i. The diagonal is therefore the trace of (8) and by equating to (9) [7],

$$tr((X')^T Rx') = tr(RH) = tr(RUSV^\top) = tr(SV^\top RU) \tag{10}$$

Let $V^\top RU = M$, where M is an orthogonal matrix for orthogonal $V^\top, R$ and U, and $tr(SM)$ is maximized if m-components equal to 1. Therefore, M is the identity matrix and the optimal rotation is given by the svd orthogonal matrices:

$$M = I = V^\top RU \rightarrow V = RU \rightarrow R = VU^\top \tag{11}$$

Finally, the translation is determined by aligning the centroids such that:

$$t = \bar{X} - R\bar{x} \tag{12}$$

The rotations and translations of each frame is stored in "rotationMatrix_all" and "translationVector_all" respectively. The function outputs "rotationMatrix" and "translationVector" for each X dataset for A, C, D, G, and H.

3.3 Pivot Calibration Algorithm

The following steps precede after finding the frame transformation of $F_G[k]$ using the EM tracking data for the EM probe as described in Section 3.2.

In order to determine the positive relative to the EM tracker base coordinate system to the dimple in the calibration post, some new variables need to be defined for all frame [k] in F_G [1]:

P_{dimple} - Fixed pivot point in EM tracker coordinates and is constant for every frame in F_G,
t_G - Tool tip location in EM probe coordinates.

Therefore, the following setup of transformation is setup to solve the least squares problem [1]:

$$\begin{aligned} P_{dimple} &= F_G \cdot t_G \\ P_{dimple} &= R \cdot t_G + t \\ R \cdot t_G - I \cdot P_{dimple} &= -t \\ [R - I][t_G; pivot\_point] &= -t \end{aligned} \tag{13}$$

This forms a least square problem in the form of $Ax = b$,
where $A = [R - I]$, $x = [t_G; pivot\_point]$ and $b = -t$.

The "pivot_calibrations.m" function uses the lsqr function to solve x, where the bottom 3 values give the coordinates of the pivot point to solve this problem.

4 Overview of Program Structure

4.1 Computing $C_{expected}$

The expected C_i location is calculated by transforming the readings of the EM markers on the calibration body in the frame of the calibration body to the EM tracker frame using the following equation.

$$C_{expected} = F_D^{-1} \cdot F_A \cdot c_i \tag{14}$$

The transformations associated with F_D and F_A are computed using the "point_cloud_registration" function, as described in 3.2.

The code associated with calculating $C_{expected}$ is located in "problem_4d" and the results of running the code are summarized in Section 6.

4.2 Computing EM Markers Probe Post Coordinates

The post coordinates of the EM marker probe, $P_{dimple} = EM_{post}$, is calculated by using the function "pivot_calibration". This function implements both the 3D point set registration algorithm to determine F_G as described in Section 3.2 and the pivot calibration algorithm as described in Section 3.3.

The code associated with computing EM_{post} is located in "problem_5" and the results of running the code are summarized in Section 6.

4.3 Computing Optical Markers Probe Post Coordinates

The post coordinates of the optical marker probe, $P_{dimple} = Optical_{post}$, is computed using both the "point_cloud_registration" and "pivot_calibration" functions. To get the optical post coordinates in the EM tracker frame, all the optical data needs to be transformed from the optical tracker frame to the EM one. This transformation F_D is calculated using the given marker data d_i and the new marker readings D_i and then applied to H_i. The transformed data is then passed into the "pivot_calibration" function to get the optical post coordinates in the EM tracker frame.

The code associated with computing $Optical_{post}$ is located in "problem_5" and the results of running the code are summarized in Section 6.

5 Verification of Results

Two main unit tests were created for testing and validating the point cloud registration and point set registration algorithms.

5.1 Point Cloud Registration Unit Tests

The unit tests used to verify the functionality of the point cloud registration algorithm described in Section 3.2 is called "registration_unit_tests.m", located in the unit tests folder of the program files.

This unit test class evaluates the functionality and accuracy of the point cloud registration function. It does so by defining a ground truth dataset consisting of a set of marker locations in the calibration object frame and applying a random transformation to get the marker locations in the tracker object frame. The unit test generates a synthetic dataset that has multiple frames of markers locations in the tracker object frame, each with their own associated random transformation.

The subclass of "matlab.unittest.TestCase" implements the test class to generate a synthetic, noise-free test dataset. A set of transformation matrices, using roll pitch and yaw for rotations and randomized translation, is stored as the known ground truth values. The test class then creates an initial set of 3D marker coordinates (x_i) within the calibration frame and applies the known transformation matrix to produce the corresponding transformed coordinates (X_i) in the tracker frame.

The same test case data for x_i and X_i is fed into the "point_cloud_registration" function for comparison to the known ground truth transformations. The difference of the the estimated rotations and translations from the "point_cloud_registration" to the known test case rotations and translations is calculated and the norm is found using the norm function. Note that using the norm function utilizes the Euclidean norm [8]. The unit test will also detect errors in the transformation matrix outside a tolerance of 1×10^{-6}.

This unit test class tests that the "point_cloud_registration" function returns accurate transformations for both a single frame and multiple frames passed into the function. It also tests for the minimum number of markers required to calculate an accurate transformation between the marker and tracker data. Running this test yielded that a minimum of 3 markers are required to calculate a transformation matrix within the defined accuracy bounds.

5.2 Pivot Calibration Unit Tests

The unit tests used to verify the functionality of the pivot calibration algorithm described in Section 3.3 is called ""pivot_calibration.m", located in the unit tests folder of the program files.

This unit test class evaluates the functionality and accuracy of the pivot calibration function. It does this by creating a synthetic ground truth dataset that consists of the marker locations in the tracker frame at each pose of the pivot calibration tool. Slight random rotations of the pivot calibration tool are introduced to generate the marker locations for each frame. The corresponding translation is also calculated to move the markers to the tracker frame and ensure that the tool tip is still located at the pivot point.

The test case data for X_i is fed into the "pivot_calibration" function for comparison to the known ground truth pivot point. The difference between the the estimated pivot to the known pivot point is calculated and the norm is found using the norm function. The norm of this difference has to be less than a tolerance of 1×10^{-6} for the unit test to pass.

After trying a couple variations of procedures for generating the randomized synthetic data, including defining a pivot point in the the tracker frame and building the marker frames around that point or doing the same in the tool frame and rotating the tool tip to various amounts, the pivot point function always converges to a pivot point of 0,0,0. It was concluded that this issue can be due to a couple sources, such as creating the randomized rotations resulting in singularities, as the issue persisted even

with using MATLAB's direct solver $x = A\backslash b$. Given more time, a more robust solution to the pivot point calibration function and unit tests would be developed to mediate the hypothesized data issues.

6 Results of Running Program - Unknown Data

The output files for unknown data h, i, j, and k are summarized in the table below. All data was extracted from output files name "pa1-unknown-x-output-1.txt".

Note that as according to the PA1 document, database h and i featured all three types of noise, including EM distortion, EM noise and OT jiggle [1]. The effects will be discussed in Section 7.

Table 1: Results for Unknown Data Sets (h, i, j, k)

File header for each unknown data set												
	pa1-unknown-h-output-1.txt			pa1-unknown-i-output-1.txt			pa1-unknown-j-output-1.txt			pa1-unknown-k-output-1.txt		
	N_C	N_{frames}	output.txt	N_C	N_{frames}	output.txt	N_C	N_{frames}	output.txt	N_C	N_{frames}	output.txt
	27.00	8.00	h-output	27.00	8.00	i-output	27.00	8.00	j-output	27.00	8.00	k-output
Estimated post position (P_x, P_y, P_z)												
EM probe pivot	190.59	200.21	183.47	210.31	192.19	197.01	198.60	205.02	188.05	185.90	200.30	207.37
Optical probe pivot	395.81	402.09	192.61	399.88	408.27	194.15	408.50	408.47	203.17	396.66	393.62	191.14
Coordinates for $C_{expected}$ (C_x, C_y, C_z)												
Frame 1	208.41	209.14	210.36	208.67	208.04	209.58	209.58	209.41	209.80	211.13	211.35	210.20
Frame 2	206.82	206.12	335.31	212.33	208.71	334.52	206.90	211.05	334.76	213.07	210.89	335.18
Frame 3	205.22	203.09	460.27	215.99	209.38	459.47	204.21	212.69	459.72	215.01	210.42	460.17
Frame 4	211.53	334.07	213.43	210.92	333.02	208.84	210.57	334.40	208.18	210.49	336.35	210.68
Frame 5	209.94	331.04	338.38	214.58	333.69	333.79	207.88	336.04	333.14	212.43	335.88	335.66
Frame 6	208.34	328.01	463.33	218.24	334.36	458.73	205.20	337.67	458.11	214.37	335.42	460.64
Frame 7	214.65	458.99	216.49	213.17	457.99	208.11	211.55	459.38	206.57	209.85	461.35	211.15
Frame 8	213.06	455.96	341.45	216.83	458.66	333.05	208.87	461.02	331.53	211.79	460.88	336.14
Frame 9	211.46	452.93	466.40	220.49	459.33	457.99	206.19	462.66	456.49	213.73	460.41	461.12
Frame 10	333.36	205.98	211.88	333.60	205.77	205.93	334.54	208.46	212.49	336.11	212.00	208.26
Frame 11	331.77	202.96	336.83	337.25	206.44	330.88	331.86	210.10	337.46	338.05	211.53	333.24
Frame 12	330.17	199.93	461.78	340.91	207.11	455.82	329.18	211.73	462.42	340.00	211.07	458.23
Frame 13	336.48	330.91	214.94	335.85	330.74	205.20	335.53	333.45	210.88	335.47	337.00	208.73
Frame 14	334.89	327.88	339.90	339.51	331.41	330.14	332.85	335.08	335.84	337.41	336.53	333.72
Frame 15	333.29	324.85	464.85	343.16	332.08	455.09	330.17	336.72	460.80	339.36	336.06	458.70
Frame 16	339.60	455.83	218.01	338.10	455.72	204.46	336.52	458.43	209.26	334.83	462.00	209.21
Frame 17	338.01	452.80	342.96	341.76	456.39	329.40	333.84	460.07	334.22	336.77	461.53	334.20
Frame 18	336.41	449.78	467.92	345.42	457.06	454.35	331.16	461.71	459.18	338.72	461.06	459.18
Frame 19	458.31	202.83	213.39	458.52	203.49	202.29	459.51	207.51	215.19	461.09	212.65	206.32
Frame 20	456.72	199.80	338.35	462.18	204.16	327.23	456.83	209.14	340.15	463.04	212.18	331.30
Frame 21	455.13	196.77	463.30	465.84	204.83	452.18	454.15	210.78	465.11	464.98	211.71	456.28
Frame 22	461.43	327.75	216.46	460.77	328.47	201.55	460.50	332.49	213.57	460.45	337.65	206.79
Frame 23	459.84	324.72	341.41	464.43	329.14	326.50	457.82	334.13	338.53	462.40	337.18	331.78
Frame 24	458.25	321.70	466.37	468.09	329.81	451.44	455.14	335.77	463.49	464.34	336.71	456.76

Frame 25	464.55	452.67	219.53	463.03	453.45	200.81	461.49	457.48	211.96	459.81	462.64	207.27
Frame 26	462.96	449.65	344.48	466.68	454.12	325.76	458.81	459.12	336.92	461.76	462.18	332.25
Frame 27	461.36	446.62	469.43	470.34	454.79	450.70	456.13	460.75	461.88	463.70	461.71	457.24
Frame 28	208.96	211.96	450.09	211.58	211.98	450.55	208.31	208.31	450.19	211.79	209.52	450.39
Frame 29	205.57	208.27	574.99	209.93	209.53	575.51	211.40	210.13	575.14	213.43	211.91	575.36
Frame 30	202.18	204.59	699.89	208.28	207.08	700.48	214.49	211.94	700.09	215.07	214.30	700.33
Frame 31	206.69	336.89	453.71	214.08	336.93	453.03	205.10	333.26	448.45	209.39	334.48	448.04
Frame 32	203.29	333.20	578.61	212.43	334.48	577.99	208.19	335.08	573.40	211.03	336.86	573.01
Frame 33	199.90	329.51	703.51	210.78	332.03	702.96	211.28	336.89	698.35	212.67	339.25	697.97
Frame 34	204.41	461.81	457.34	216.58	461.88	455.51	201.90	458.21	446.72	206.99	459.43	445.68
Frame 35	201.01	458.13	582.24	214.93	459.43	580.47	204.99	460.02	571.67	208.63	461.82	570.65
Frame 36	197.62	454.44	707.14	213.28	456.98	705.44	208.08	461.84	696.61	210.27	464.20	695.62
Frame 37	333.90	214.14	453.55	336.54	209.45	452.15	333.23	211.47	447.06	336.76	211.89	448.71
Frame 38	330.50	210.45	578.45	334.89	207.00	577.11	336.32	213.29	572.00	338.39	214.28	573.68
Frame 39	327.11	206.76	703.35	333.24	204.55	702.08	339.41	215.11	696.95	340.03	216.66	698.64
Frame 40	331.62	339.06	457.17	339.04	334.40	454.63	330.03	336.42	445.32	334.36	336.84	446.35
Frame 41	328.22	335.38	582.07	337.39	331.95	579.59	333.12	338.24	570.27	335.99	339.23	571.32
Frame 42	324.83	331.69	706.97	335.74	329.50	704.56	336.20	340.05	695.22	337.63	341.62	696.29
Frame 43	329.34	463.99	460.80	341.54	459.35	457.11	326.82	461.37	443.58	331.96	461.80	444.00
Frame 44	325.95	460.30	585.70	339.89	456.90	582.07	329.91	463.18	568.53	333.59	464.19	568.97
Frame 45	322.55	456.62	710.60	338.24	454.45	707.04	333.00	465.00	693.48	335.23	466.57	693.93
Frame 46	458.83	216.32	457.01	461.51	206.92	453.75	458.15	214.64	443.92	461.72	214.26	447.03
Frame 47	455.44	212.63	581.91	459.86	204.47	578.71	461.24	216.45	568.87	463.36	216.65	571.99
Frame 48	452.04	208.94	706.81	458.21	202.02	703.68	464.33	218.27	693.82	465.00	219.03	696.96
Frame 49	456.55	341.24	460.63	464.01	331.87	456.23	454.95	339.58	442.18	459.32	339.21	444.67
Frame 50	453.16	337.55	585.53	462.36	329.42	581.19	458.04	341.40	567.13	460.96	341.60	569.64
Frame 51	449.76	333.87	710.43	460.71	326.97	706.16	461.13	343.22	692.08	462.60	343.99	694.60
Frame 52	454.27	466.17	464.26	466.50	456.82	458.71	451.74	464.53	440.45	456.92	464.17	442.32
Frame 53	450.88	462.48	589.16	464.86	454.37	583.67	454.83	466.35	565.40	458.56	466.55	567.28
Frame 54	447.49	458.79	714.06	463.21	451.92	708.64	457.92	468.16	690.34	460.20	468.94	692.25
Frame 55	209.66	451.44	210.39	208.72	450.10	208.61	209.30	448.73	208.96	210.63	451.77	209.23
Frame 56	210.12	451.84	335.39	207.88	448.50	333.60	210.97	449.63	333.95	212.51	455.48	334.16
Frame 57	210.58	452.25	460.39	207.05	446.90	458.58	212.64	450.53	458.93	214.38	459.20	459.09
Frame 58	207.12	576.41	210.00	210.20	575.09	210.22	207.31	573.71	208.09	211.32	576.72	205.50
Frame 59	207.58	576.82	335.00	209.36	573.48	335.21	208.98	574.61	333.07	213.19	580.43	330.43
Frame 60	208.04	577.22	460.00	208.52	571.88	460.20	210.65	575.51	458.06	215.07	584.14	455.37
Frame 61	204.57	701.39	209.61	211.67	700.07	211.83	205.32	698.69	207.22	212.00	701.66	201.78

Frame 62	205.03	701.79	334.60	210.83	698.46	336.82	206.99	699.59	332.20	213.88	705.37	326.71
Frame 63	205.50	702.20	459.60	209.99	696.86	461.81	208.66	700.49	457.19	215.75	709.08	451.64
Frame 64	334.64	453.98	209.93	333.71	448.62	209.43	334.27	450.71	207.28	335.61	451.03	207.37
Frame 65	335.10	454.39	334.92	332.87	447.02	334.42	335.94	451.61	332.26	337.49	454.74	332.30
Frame 66	335.56	454.79	459.92	332.03	445.41	459.40	337.61	452.50	457.25	339.37	458.45	457.23
Frame 67	332.09	578.96	209.53	335.18	573.60	211.04	332.28	575.69	206.40	336.30	575.97	203.65
Frame 68	332.55	579.36	334.53	334.35	572.00	336.03	333.95	576.59	331.39	338.18	579.69	328.58
Frame 69	333.01	579.76	459.53	333.51	570.40	461.02	335.62	577.49	456.38	340.05	583.40	453.51
Frame 70	329.55	703.93	209.14	336.66	698.58	212.65	330.29	700.67	205.53	336.99	700.92	199.93
Frame 71	330.01	704.33	334.14	335.82	696.98	337.64	331.96	701.57	330.52	338.86	704.63	324.86
Frame 72	330.47	704.74	459.13	334.98	695.38	462.63	333.63	702.47	455.50	340.74	708.34	449.79
Frame 73	459.61	456.53	209.46	458.70	447.14	210.25	459.24	452.69	205.59	460.60	450.29	205.52
Frame 74	460.07	456.93	334.45	457.86	445.53	335.24	460.91	453.58	330.58	462.47	454.00	330.45
Frame 75	460.53	457.33	459.45	457.02	443.93	460.22	462.58	454.48	455.56	464.35	457.71	455.38
Frame 76	457.06	581.50	209.06	460.17	572.12	211.86	457.25	577.67	204.72	461.28	575.23	201.80
Frame 77	457.53	581.90	334.06	459.33	570.51	336.85	458.92	578.57	329.71	463.16	578.94	326.73
Frame 78	457.99	582.31	459.06	458.50	568.91	461.84	460.59	579.46	454.69	465.04	582.66	451.66
Frame 79	454.52	706.47	208.67	461.65	697.10	213.47	455.26	702.65	203.85	461.97	700.18	198.07
Frame 80	454.98	706.88	333.67	460.81	695.50	338.46	456.93	703.55	328.83	463.85	703.89	323.00
Frame 81	455.44	707.28	458.66	459.97	693.89	463.45	458.60	704.44	453.82	465.72	707.60	447.93
Frame 82	208.92	449.63	448.10	209.29	450.56	451.50	211.55	449.95	450.22	210.31	451.27	448.39
Frame 83	206.06	450.10	573.07	209.00	449.31	576.49	213.86	453.45	575.15	207.10	449.13	573.33
Frame 84	203.20	450.56	698.03	208.71	448.05	701.49	216.16	456.94	700.08	203.90	446.99	698.27
Frame 85	209.50	574.63	447.65	211.39	575.54	452.76	209.17	574.88	446.77	208.71	576.24	450.48
Frame 86	206.64	575.09	572.61	211.09	574.28	577.75	211.47	578.38	571.70	205.51	574.10	575.42
Frame 87	203.79	575.56	697.58	210.80	573.03	702.74	213.78	581.87	696.63	202.30	571.96	700.36
Frame 88	210.09	699.62	447.19	213.48	700.51	454.02	206.79	699.81	443.32	207.12	701.21	452.58
Frame 89	207.23	700.09	572.16	213.19	699.26	579.01	209.09	703.31	568.25	203.91	699.07	577.52
Frame 90	204.37	700.56	697.12	212.90	698.01	704.00	211.39	706.80	693.18	200.70	696.94	702.46
Frame 91	333.88	449.05	450.96	334.27	448.46	451.77	336.51	452.27	447.85	335.26	452.81	451.62
Frame 92	331.03	449.52	575.93	333.98	447.21	576.76	338.81	455.77	572.78	332.05	450.67	576.56
Frame 93	328.17	449.99	700.89	333.69	445.96	701.76	341.12	459.26	697.71	328.85	448.53	701.50
Frame 94	334.47	574.05	450.51	336.37	573.44	453.03	334.13	577.20	444.40	333.66	577.78	453.72
Frame 95	331.61	574.52	575.47	336.08	572.19	578.02	336.43	580.70	569.33	330.46	575.64	578.66
Frame 96	328.75	574.99	700.44	335.78	570.93	703.01	338.73	584.19	694.26	327.25	573.51	703.60
Frame 97	335.05	699.05	450.05	338.46	698.42	454.29	331.74	702.13	440.95	332.06	702.76	455.81
Frame 98	332.20	699.52	575.02	338.17	697.16	579.28	334.04	705.62	565.88	328.86	700.62	580.76

Frame 99	329.34	699.98	699.99	337.88	695.91	704.27	336.35	709.12	690.81	325.65	698.48	705.70
Frame 100	458.85	448.48	453.82	459.26	446.37	452.04	461.47	454.59	445.48	460.21	454.35	454.85
Frame 101	455.99	448.95	578.79	458.96	445.11	577.03	463.77	458.08	570.41	457.00	452.22	579.79
Frame 102	453.13	449.41	703.75	458.67	443.86	702.03	466.07	461.58	695.34	453.79	450.08	704.73
Frame 103	459.44	573.48	453.37	461.35	571.34	453.30	459.08	579.52	442.03	458.61	579.33	456.95
Frame 104	456.58	573.94	578.33	461.06	570.09	578.29	461.38	583.01	566.96	455.40	577.19	581.89
Frame 105	453.72	574.41	703.30	460.77	568.84	703.29	463.69	586.51	691.89	452.20	575.05	706.83
Frame 106	460.02	698.47	452.91	463.44	696.32	454.56	456.70	704.45	438.58	457.01	704.30	459.05
Frame 107	457.16	698.94	577.88	463.15	695.07	579.55	459.00	707.94	563.51	453.81	702.16	583.99
Frame 108	454.30	699.41	702.85	462.86	693.81	704.54	461.30	711.44	688.44	450.60	700.02	708.93
Frame 109	451.11	208.22	210.74	450.70	211.81	211.34	451.11	209.58	211.74	450.96	209.37	211.65
Frame 110	451.35	211.22	335.70	447.86	210.35	336.30	454.70	212.45	336.65	450.15	209.60	336.64
Frame 111	451.60	214.23	460.67	445.02	208.88	461.26	458.29	215.33	461.57	449.33	209.82	461.64
Frame 112	452.62	333.17	207.73	453.68	336.77	212.87	450.31	334.55	208.89	447.72	334.33	211.40
Frame 113	452.87	336.18	332.69	450.84	335.30	337.83	453.90	337.42	333.80	446.91	334.56	336.40
Frame 114	453.12	339.18	457.66	448.00	333.84	462.79	457.49	340.29	458.72	446.09	334.78	461.39
Frame 115	454.14	458.13	204.72	456.66	461.72	214.41	449.51	459.51	206.03	444.48	459.29	211.15
Frame 116	454.39	461.13	329.69	453.82	460.26	339.37	453.10	462.38	330.95	443.67	459.51	336.15
Frame 117	454.64	464.14	454.65	450.98	458.79	464.33	456.68	465.26	455.87	442.85	459.74	461.15
Frame 118	576.10	206.69	210.53	575.63	208.80	214.15	576.06	210.30	208.13	575.91	212.62	212.45
Frame 119	576.34	209.70	335.49	572.79	207.33	339.10	579.65	213.17	333.05	575.10	212.84	337.45
Frame 120	576.59	212.71	460.46	569.95	205.87	464.06	583.23	216.05	457.96	574.29	213.07	462.45
Frame 121	577.61	331.65	207.52	578.61	333.75	215.68	575.26	335.26	205.28	572.68	337.57	212.21
Frame 122	577.86	334.65	332.48	575.77	332.29	340.64	578.85	338.14	330.20	571.86	337.80	337.20
Frame 123	578.11	337.66	457.45	572.93	330.82	465.60	582.43	341.01	455.11	571.05	338.02	462.20
Frame 124	579.13	456.60	204.51	581.59	458.71	217.21	574.46	460.23	202.43	569.44	462.53	211.96
Frame 125	579.38	459.61	329.48	578.75	457.24	342.17	578.04	463.10	327.35	568.62	462.76	336.96
Frame 126	579.63	462.61	454.44	575.91	455.78	467.13	581.63	465.98	452.26	567.81	462.98	461.95
Frame 127	701.09	205.17	210.32	700.56	205.78	216.95	701.01	211.02	204.53	700.87	215.86	213.26
Frame 128	701.33	208.18	335.28	697.72	204.32	341.91	704.59	213.89	329.45	700.06	216.08	338.26
Frame 129	701.58	211.18	460.25	694.88	202.85	466.87	708.18	216.76	454.36	699.24	216.31	463.25
Frame 130	702.61	330.12	207.31	703.54	330.74	218.48	700.20	335.98	201.68	697.63	340.81	213.01
Frame 131	702.85	333.13	332.28	700.70	329.27	343.44	703.79	338.86	326.59	696.82	341.04	338.01
Frame 132	703.10	336.14	457.24	697.86	327.81	468.40	707.38	341.73	451.51	696.00	341.27	463.01
Frame 133	704.12	455.08	204.30	706.52	455.69	220.02	699.40	460.95	198.83	694.39	465.77	212.77
Frame 134	704.37	458.08	329.27	703.68	454.23	344.98	702.99	463.82	323.74	693.58	466.00	337.76
Frame 135	704.62	461.09	454.23	700.84	452.76	469.94	706.58	466.69	448.66	692.77	466.22	462.76

Frame 136	450.23	208.18	450.60	449.51	209.92	448.53	450.74	211.04	451.65	448.21	209.08	450.44
Frame 137	447.24	207.06	575.56	451.57	206.65	573.47	450.08	210.87	576.65	450.81	205.54	575.36
Frame 138	444.25	205.93	700.51	453.63	203.37	698.41	449.42	210.70	701.65	453.41	202.00	700.28
Frame 139	452.18	333.16	451.77	452.81	334.84	451.75	448.42	336.02	451.81	444.53	333.97	454.05
Frame 140	449.19	332.04	576.73	454.87	331.56	576.69	447.76	335.85	576.81	447.13	330.43	578.98
Frame 141	446.20	330.91	701.69	456.92	328.29	701.63	447.10	335.68	701.81	449.73	326.89	703.90
Frame 142	454.14	458.14	452.94	456.11	459.75	454.97	446.09	461.00	451.97	440.84	458.86	457.67
Frame 143	451.15	457.02	577.90	458.17	456.48	579.91	445.43	460.83	576.97	443.44	455.33	582.59
Frame 144	448.16	455.89	702.86	460.22	453.20	704.85	444.77	460.66	701.96	446.04	451.79	707.51
Frame 145	575.18	206.20	453.57	574.45	206.68	446.39	575.72	213.37	452.31	573.13	212.84	447.94
Frame 146	572.19	205.08	578.53	576.51	203.40	571.33	575.06	213.20	577.31	575.73	209.30	572.87
Frame 147	569.20	203.95	703.49	578.57	200.13	696.27	574.40	213.03	702.31	578.33	205.76	697.79
Frame 148	577.13	331.18	454.74	577.75	331.59	449.61	573.39	338.35	452.47	569.44	337.73	451.56
Frame 149	574.14	330.06	579.70	579.81	328.32	574.55	572.73	338.18	577.47	572.04	334.19	576.48
Frame 150	571.15	328.93	704.66	581.86	325.04	699.49	572.08	338.00	702.47	574.65	330.65	701.40
Frame 151	579.09	456.16	455.91	581.05	456.51	452.83	571.07	463.32	452.63	565.76	462.62	455.17
Frame 152	576.10	455.04	580.87	583.11	453.23	577.77	570.41	463.15	577.63	568.36	459.09	580.10
Frame 153	573.11	453.91	705.83	585.16	449.96	702.71	569.75	462.98	702.63	570.96	455.55	705.02
Frame 154	700.13	204.22	456.54	699.39	203.43	444.25	700.69	215.69	452.97	698.05	216.60	445.45
Frame 155	697.14	203.10	581.50	701.45	200.16	569.19	700.04	215.52	577.97	700.65	213.06	570.37
Frame 156	694.15	201.97	706.46	703.50	196.88	694.13	699.38	215.35	702.97	703.25	209.52	695.29
Frame 157	702.08	329.20	457.71	702.69	328.35	447.47	698.37	340.67	453.13	694.36	341.49	449.06
Frame 158	699.09	328.07	582.67	704.75	325.07	572.41	697.71	340.50	578.13	696.96	337.95	573.99
Frame 159	696.10	326.95	707.63	706.80	321.80	697.35	697.05	340.33	703.13	699.56	334.41	698.91
Frame 160	704.04	454.18	458.88	705.99	453.26	450.69	696.04	465.65	453.29	690.68	466.38	452.68
Frame 161	701.05	453.05	583.84	708.05	449.99	575.63	695.38	465.48	578.29	693.28	462.85	577.60
Frame 162	698.06	451.93	708.80	710.10	446.71	700.57	694.73	465.31	703.29	695.88	459.31	702.52
Frame 163	450.49	448.57	210.24	449.47	448.44	211.60	448.66	449.27	208.25	450.76	451.82	211.49
Frame 164	452.39	449.52	335.22	448.86	450.05	336.59	451.61	451.54	333.19	449.32	449.59	336.46
Frame 165	454.29	450.46	460.20	448.26	451.65	461.58	454.57	453.81	458.14	447.88	447.36	461.44
Frame 166	453.96	573.52	209.24	451.71	573.41	210.02	447.35	574.24	206.01	452.59	576.79	213.74
Frame 167	455.86	574.46	334.22	451.10	575.02	335.00	450.30	576.51	330.95	451.15	574.56	338.72
Frame 168	457.76	575.41	459.21	450.49	576.62	459.99	453.26	578.78	455.90	449.71	572.33	463.69
Frame 169	457.43	698.47	208.24	453.94	698.38	208.43	446.04	699.21	203.77	454.41	701.75	216.00
Frame 170	459.33	699.41	333.23	453.34	699.99	333.41	448.99	701.48	328.71	452.98	699.52	340.97
Frame 171	461.23	700.36	458.21	452.73	701.59	458.40	451.95	703.75	453.66	451.54	697.29	465.94
Frame 172	575.42	445.08	208.37	574.45	446.22	212.24	573.62	450.52	205.27	575.74	449.97	212.90

Frame 173	577.32	446.03	333.35	573.84	447.82	337.23	576.57	452.79	330.21	574.30	447.74	337.87
Frame 174	579.22	446.98	458.33	573.23	449.42	462.22	579.53	455.06	455.16	572.86	445.51	462.84
Frame 175	578.89	570.03	207.37	576.69	571.19	210.65	572.31	575.50	203.03	577.57	574.93	215.15
Frame 176	580.80	570.98	332.35	576.08	572.79	335.64	575.26	577.77	327.98	576.13	572.70	340.12
Frame 177	582.70	571.92	457.33	575.47	574.39	460.63	578.22	580.04	452.92	574.69	570.47	465.09
Frame 178	582.37	694.98	206.37	578.92	696.16	209.06	571.00	700.47	200.79	579.39	699.90	217.40
Frame 179	584.27	695.93	331.35	578.31	697.76	334.05	573.95	702.74	325.74	577.95	697.67	342.37
Frame 180	586.17	696.87	456.33	577.71	699.36	459.04	576.91	705.01	450.68	576.52	695.44	467.34
Frame 181	700.36	441.60	206.49	699.43	443.99	212.88	698.58	451.78	202.29	700.72	448.11	214.30
Frame 182	702.26	442.54	331.48	698.82	445.59	337.87	701.53	454.05	327.24	699.28	445.88	339.28
Frame 183	704.16	443.49	456.46	698.21	447.19	462.85	704.49	456.32	452.18	697.84	443.65	464.25
Frame 184	703.83	566.55	205.50	701.66	568.96	211.29	697.27	576.75	200.05	702.54	573.08	216.55
Frame 185	705.73	567.49	330.48	701.06	570.56	336.28	700.22	579.02	325.00	701.11	570.85	341.53
Frame 186	707.63	568.44	455.46	700.45	572.16	461.26	703.18	581.29	449.94	699.67	568.62	466.50
Frame 187	707.30	691.49	204.50	703.90	693.93	209.70	695.96	701.73	197.81	704.37	698.05	218.81
Frame 188	709.20	692.44	329.48	703.29	695.53	334.69	698.91	704.00	322.76	702.93	695.82	343.78
Frame 189	711.10	693.39	454.46	702.69	697.13	459.67	701.86	706.27	447.70	701.49	693.59	468.75
Frame 190	448.12	451.60	448.04	448.63	450.57	449.56	449.52	449.21	449.18	448.09	450.21	452.00
Frame 191	448.27	450.52	573.04	449.40	452.67	574.54	452.98	450.73	574.12	449.44	453.78	576.94
Frame 192	448.41	449.43	698.03	450.16	454.76	699.52	456.45	452.25	699.07	450.80	457.35	701.88
Frame 193	446.09	576.58	449.13	449.00	575.56	447.47	447.24	574.18	447.73	444.87	575.12	448.46
Frame 194	446.23	575.50	574.13	449.77	577.65	572.45	450.71	575.70	572.67	446.22	578.69	573.41
Frame 195	446.38	574.41	699.12	450.53	579.74	697.43	454.17	577.22	697.61	447.57	582.26	698.35
Frame 196	444.05	701.56	450.22	449.38	700.54	445.37	444.97	699.16	446.27	441.65	700.03	444.93
Frame 197	444.20	700.47	575.22	450.14	702.63	570.35	448.43	700.67	571.21	443.00	703.60	569.87
Frame 198	444.34	699.39	700.21	450.91	704.72	695.33	451.90	702.19	696.16	444.35	707.17	694.82
Frame 199	573.11	453.64	447.92	573.63	450.19	448.81	574.45	451.45	445.69	573.04	453.39	450.55
Frame 200	573.25	452.55	572.91	574.39	452.28	573.79	577.92	452.97	570.63	574.39	456.96	575.50
Frame 201	573.40	451.47	697.91	575.16	454.38	698.77	581.38	454.48	695.57	575.75	460.53	700.44
Frame 202	571.07	578.62	449.01	574.00	575.17	446.71	572.17	576.42	444.23	569.82	578.30	447.02
Frame 203	571.22	577.53	574.00	574.77	577.26	571.69	575.64	577.94	569.18	571.17	581.87	571.96
Frame 204	571.36	576.44	699.00	575.53	579.36	696.67	579.11	579.45	694.12	572.53	585.44	696.91
Frame 205	569.04	703.60	450.10	574.37	700.15	444.61	569.90	701.39	442.78	566.60	703.21	443.49
Frame 206	569.18	702.51	575.09	575.14	702.25	569.59	573.36	702.91	567.72	567.95	706.78	568.43
Frame 207	569.32	701.42	700.09	575.90	704.34	694.57	576.83	704.42	692.66	569.30	710.35	693.37
Frame 208	698.09	455.68	447.79	698.63	449.80	448.05	699.38	453.68	442.20	697.99	456.58	449.11
Frame 209	698.24	454.59	572.78	699.39	451.90	573.03	702.85	455.20	567.14	699.35	460.14	574.05

Frame 210	698.38	453.50	697.78	700.16	453.99	698.01	706.31	456.72	692.08	700.70	463.71	698.99
Frame 211	696.05	580.66	448.88	699.00	574.79	445.95	697.11	578.65	440.74	694.77	581.48	445.58
Frame 212	696.20	579.57	573.87	699.76	576.88	570.93	700.57	580.17	565.68	696.12	585.05	570.52
Frame 213	696.34	578.48	698.87	700.53	578.97	695.91	704.04	581.69	690.63	697.48	588.62	695.46
Frame 214	694.02	705.64	449.97	699.37	699.77	443.86	694.83	703.62	439.29	691.55	706.39	442.05
Frame 215	694.16	704.55	574.96	700.14	701.86	568.84	698.30	705.14	564.23	692.90	709.96	566.99
Frame 216	694.31	703.46	699.96	700.90	703.95	693.82	701.76	706.66	689.17	694.26	713.53	691.93

7 Error Analysis

Auxiliary data files are created for each debug dataset as part of the output folder, named "pa1-debug-x-auxiliary1.txt" for x files a to g and "pa1-unknown-x-auxiliary1.txt" for x files h to k. The function "create_auxiliary_file.m", located in the error analysis folder, compares the calculated EM pivot post coordinates, optical pivot post coordinates, and $C_{expected}$ values to the actual dataset values. The output file is formatted similarly to the ones provided in the program template.

7.1 Debug Data for Specified Noise

This section will focus on debug files b, c and d. As summarized in the PA1 document, dataset b has EM noise, database c has EM distortion, and database d has OT jiggle. These datasets will allow isolated analysis of the effects of each type of error.

EM Noise represents random fluctuations present along each individual measurement along each coordinate axis. EM distortion refers to a systematic error that varies with position relative to the EM tracking device. The OT jiggle corresponds to small physical movements or vibrations of the optical tracking base unit that occur between successive data frames. The table below summarizes the differences due to different types of error.

Table 2: Summary of database b, c and d error effects on $C_{expected}$

Dataset	**Mean Difference**	**Mean Difference Norm**	**Max Difference Norm**
A - None	0, 0, 0	0	0.01
B - EM Noise	-0.02, 0.00, 0.03	0.46	0.79
C - EM Distortion	1.03, 0.75, -0.44	3.51	7.09
D - OT Jiggle	0.00, 0.00, 0.00	0.01	0.03
E - EM Noise + OT Jiggle	1.01, -0.72, 1.09	6.49	16.44
F - All	0.94, 1.05, 1.09	6.66	17.47
G - All	-0.74, -0.35, -1.86	6.55	21.32
H - Unknown	0.78, -2.26, -3.09	19.98	38.53
I - Unknown	1.29, 1.14, -1.68	6.64	14.2
J - Unknown	0.53, -0.41, 0.84	4.38	10.82
K - Unknown	-0.92, 0.87, -0.77	5.93	15.00

The auxiliary file creation function has three main metrics to compare the actual marker positions (C_{actual}) measured by the EM tracking system with the expected marker positions ($C_{expected}$) that were calculated based on calibration data. The difference between the two sets is as follows:

$$C_{error} = C_{actual} - C_{expected} \tag{15}$$

for coordinates in X, Y and Z for each frame.

The mean difference is the average signed offset between the measured and expected positions along each coordinate axis (X, Y, Z) such that:

$$\text{Mean Difference} = \frac{1}{N}\sum_{i=1}^{N} C_{error,i} \tag{16}$$

This value represents the average offset between coordinate datasets and indicating bias in the EM measurements along any axis. It is noted that the EM distortion in dataset c has the largest deviations in all three coordinate axes. EM noise in dataset b has little deviations in the X and Z axes, while OT jiggle in dataset d has no deviations due to associations with the optical tracking base only.

The mean difference norm finds the Euclidean norm of the position error of each point:

$$|C_{error,i}| = \sqrt{(\Delta x)^2 + (\Delta y)^2 + (\Delta z)^2}$$

$$\text{Mean Difference Norm} = \frac{1}{N}\sum_{i=1}^{N} |C_{error,i}|$$

The single scalar value of this norm represents the average magnitude of positional error across all markers and frames, regardless of direction. This measurement provides the overall accuracy of the EM tracking system, with smaller values indicating more precise tracking. Similarly to the mean difference, the EM distortion has the largest deviation at 3.51. The impact of EM noise on the dataset b still shows significant deviation at 0.46. Both errors need to be corrected for a more effective system. Note again that there is very little deviation in the dataset d due to association with the optical system.

The max difference norm is the maximum Euclidean norm of the errors to indicate the worse-case deviation of the measured and expected positions. It can flag occasional outliers or system instability of marker readings with significant tracking error.

$$\text{Max Difference Norm} = \max_i |C_{error,i}| \tag{17}$$

The maximum continues to be significant deviation in dataset c at 7.09 from the EM distortion error.

By analyzing datasets b, c and d, the team is able to isolate and analyze each type of error and its effects on deviating the expected and actual values of C. Especially the EM distortion on dataset c created significant deviations as visualized below.

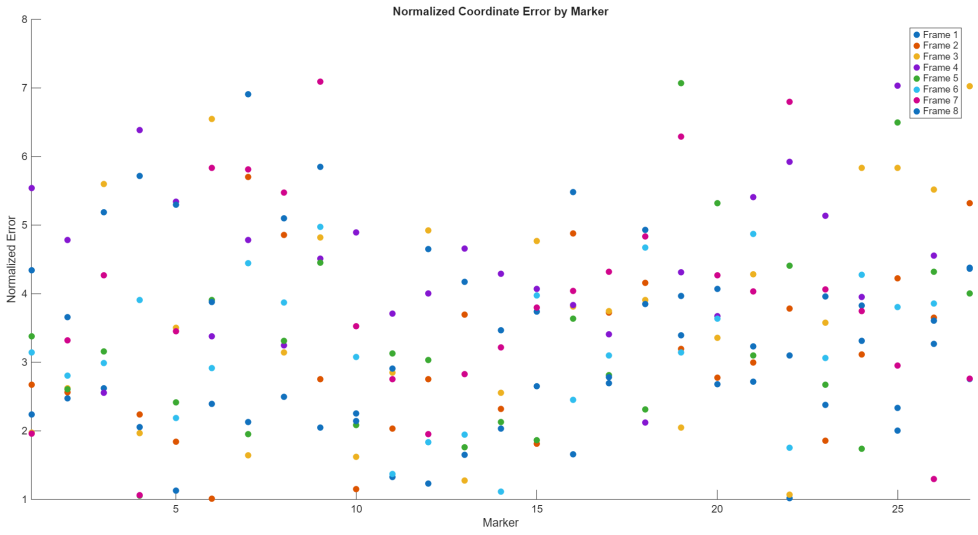

Figure 3: Normalized Error by Marker and Frame for Dataset C

Table 2 summarizes errors in all dataset files and how the combination of errors drastically fluctuate the data. There is even more accumulated error that must be corrected, which will be discussed in Section 7.3.

7.2 Convergence in lsqr

Refer to Section 2.2 for the mathematical background of the lsqr function. The lsqr function provides an estimate of the relative residual during the iterative process to converge to a solution, which minimizes the Euclidean norm of the residual in equation 1.

However, in practice, the final relative residual can deviate from the specified tolerance, as observed in the datasets tabulated below. To verify that these deviations are inherent to the system's datasets, tests were conducted by using MATLAB's direct solver $x = A\backslash b$, which produced the same residuals as the lsqr function. Therefore, with increasingly large deviations and errors in the datasets, the convergence of the least squares solution is fundamentally limited by the structure and condition of the system rather than the iterative solver.

The next section will discuss briefly the future work for mediating these distortions and improving the resultant least squares solutions.

Table 3: Summary of Relative Residual of EM and Optical Post Pivot Coordinates

	Relative Residual	
Dataset	EM Post Pivot	Optical Post Pivot
a	8.50E-06	6.70E-06
b	9.10E-06	6.80E-06
c	1.50E-03	3.60E-06
d	1.00E-05	8.30E-06
e	8.90E-03	1.10E-05
f	4.90E-03	8.30E-06
g	7.80E-03	9.60E-06
h	8.00E-03	1.30E-05
i	6.30E-03	9.60E-06
j	4.50E-03	3.30E-06
k	4.00E-03	1.10E-05

7.3 Future Work

In the next assignment, the team will implement 3D calibration techniques for distortion on datasets X_i, prior to implementing point cloud registration and finding the transformation matrices. The raw data will be scaled to box to created a scaled correction function in unit cubes. The 5th Bernstein polynomial will scale the normalized data by the tensor of calibration coefficients to provide the corrected data for X_i.

8 Work Distribution

The distribution of the work was shared between both team members. Shreya and Yvonne worked together on the mathematical approach and understanding the setup as described in Figures 1 and 2.

Shreya focused on functions used to read data files, the point cloud registration function, unit testing files, and error analysis files. Yvonne focused on the point set registration algorithm, pivot calibration algorithm, and translating the team's work into the report.

References

[1] R. Taylor, "Programming assignment 1 2," 2025. Accessed: 2025-09-18.

[2] The MathWorks, Inc., "Linear algebra - symbolic math toolbox documentation," 2025. Accessed: 2025-10-03.

[3] The MathWorks, Inc., "svd - singular value decomposition," 2025. Accessed: 2025-10-03.

[4] G. Gundersen, "A non-technical introduction to svd," 2018. Accessed: 2025-10-03.

[5] J. Shi, "Arun's method for 3d registration," 2018. Accessed: 2025-09-21.

[6] The MathWorks, Inc., "lsqr - solve system of linear equations: least-squares method," 2025. Accessed: 2025-10-01.

[7] O. Sorkine-Hornung and M. Rabinovich, "Least-squares rigid motion using svd." Technical Report, ETH Zurich, 2017. Accessed: 2025-09-21.

[8] The MathWorks, Inc., "norm - vector and matrix norms," 2025. Accessed: 2025-10-06.